

# Deep Reinforcement Learning for Optimal Power Flow with Renewables Using Graph Information

Jinhao Li<sup>1</sup>, Ruichang Zhang<sup>2</sup>, Hao Wang<sup>3</sup>, Zhi Liu<sup>4</sup>, Hongyang Lai<sup>1</sup>, Yanru Zhang<sup>2,5</sup>

<sup>1</sup>School of Mechanical and Electrical Engineering, University of Electronic Science and Technology of China, China

<sup>2</sup>School of Computer Science and Engineering, University of Electronic Science and Technology of China, China

<sup>3</sup>Department of Data Science and Artificial Intelligence, Monash University, Australia

<sup>4</sup>Department of Computer and Network Engineering, University of Electro-Communications, Japan

<sup>5</sup>Shenzhen Institute of Advanced Study, University of Electronic Science and Technology of China, China

Email: jinhaoli@std.uestc.edu.cn, yanruzhang@uestc.edu.cn

**Abstract**—Renewable energy resources (RERs) have been increasingly integrated into large-scale distributed power systems. Considering uncertainties and voltage fluctuation issues introduced by RERs, in this paper, we propose a deep reinforcement learning (DRL)-based strategy leveraging spatial-temporal (ST) graphical information of power systems, to dynamically search for the optimal operation, i.e., optimal power flow (OPF), of power systems with a high uptake of RERs. Specifically, we formulate the OPF problem as a multi-objective optimization problem considering generation cost, voltage fluctuation, and transmission loss, and employ deep deterministic policy gradient (DDPG) to learn an optimal allocation strategy for OPF. Moreover, given that the nodes in power systems are self-correlated and interrelated in temporal and spatial views, we develop a multi-grained attention-based spatial-temporal graph convolution network (MG-ASTGCN) for extracting ST graphical correlations and features, aiming to provide prior knowledge of power systems for its sequential DDPG algorithm to more effectively solve OPF. We validate our algorithm on modified IEEE 33, 69, and 118-bus radial distribution systems and demonstrate that our algorithm outperforms other benchmark algorithms. Our experimental results also reveal that our MG-ASTGCN can significantly accelerate DDPG’s training process and performance in solving OPF.

**Index Terms**—Optimal power flow (OPF), renewable energy resources (RERs), deep reinforcement learning (DRL), graph convolution, attention mechanism.

## I. INTRODUCTION

There has been an exponential growth of distributed renewable energy resources (RERs) in power systems for mitigating global climate change and providing affordable electricity to customers [1]. Although the adoption of RERs in conventional power systems offers various benefits, such as decarbonizing the electricity market and reducing the energy supply costs, the integration of RERs into power systems, at the same time, poses significant challenges due to their intermittent nature [2].

One of the major challenges is that the RERs lead to consecutive and fast changes of the optimal operating point in power systems [3]. Calculating the optimal operating point is known as solving the optimal power flow (OPF) problem, which is formulated to minimize the cost of power generation while satisfying power systems’ operating constraints [4]. Various external factors, such as changes in solar irradiation and wind velocity, cause stochastic and non-dispatchable generation of RERs, inevitably leading to continuous changes

of power flow. Moreover, since the number of newly installed RER systems cannot be accurately predicted, several technical issues can also occur, such as voltage fluctuations and harmonic distortions, threatening power systems’ stability and can cause potential economic losses. These challenges motivate our work to take both uncertainty and stability factors into consideration and to optimize power flow efficiently for power systems with a high penetration of RERs.

The existing studies on solving OPF can be briefly categorized into three classes—numerical, model-based, and deep-learning algorithms, which all suffer from significant drawbacks. 1) Numerical methods, such as Gauss-Seidel and Newton-Raphson algorithms, are extremely difficult to converge because of the uncertainties brought by RERs when solving OPF [5]; 2) Model-based algorithms can be less effective when it comes to large-scale power systems, as most of model-based methods are highly dependent on accurate knowledge of given power systems [6]. Besides, they are also sensitive to initialization values and can trap into local optimum [7]; 3) Deep-learning methods require a large amount of historical data to train an accurate deep-learning model [8], becoming a barrier to the adoption of deep-learning methods. In particular, it is inherently challenging for deep-learning methods to react quickly to dynamic changes of optimal operating point.

To overcome the aforementioned drawbacks, this paper introduces deep reinforcement learning (DRL) to solve the OPF problem. DRL is well suitable to capture the dynamic features in RERs-rich power systems, and thus powerful in solving the OPF problem. However, learning a stable and well-performed DRL-based strategy is time-consuming due to its slow convergence in complex systems, such as OPF of power systems [9]. How to extract effective information from complex power systems becomes an essential to accelerate the learning of DRL algorithms. Due to the strong coupling in OPF problems, the nodes (e.g., buses) in power systems are self-correlated and interrelated in temporal and spatial views, containing a prior knowledge of power systems that can play a significant role in assisting the DRL model to solve OPF more effectively. Existing studies did not capture such effective features, e.g., the spatial-temporal (ST) information, about power flows. Therefore, we develop a multi-grained attention-based spatial-temporal convolution network (MG-ASTGCN)

to extract ST correlations through attention mechanism and ST features through graph convolution, providing effective information for the DRL algorithm.

The main contributions of our work are summarized as follows.

- *Solving OPF by DRL*: We propose a DRL-based strategy using DDPG leveraging ST graphical information to solve OPF with a high renewable penetration in power systems. Our method can dynamically dispatch power flow, search for the optimal operating point, and quickly respond to uncertainties brought by RERs. Our DRL algorithm demonstrated to outperform benchmark algorithms, such as harris hawk optimization (HHO) and grey wolf optimization (GWO), through simulations.
- *Extraction of Spatial and Temporal Information*: We develop the multi-grained attention-based spatial-temporal graph convolution network (MG-ASTGCN) to fully extract ST information in dynamic power flow, where the attention mechanism and graph convolution are adopted for mining ST correlations and features, respectively. Additionally, given that the power flow exhibits periodic patterns in different time scales, we construct mutli-grained power flow time-series to capture multi-scale ST information. MG-ASTGCN can provide global prior knowledge of power systems for the DRL algorithm to accelerate its convergence in solving OPF.

## II. SYSTEM MODEL

We consider a distributed power distribution network whose power generation is supported by fuel energy, wind power, and solar PV power. Wind and solar PV power are regarded as the most representative RERs with the largest installed capacities [1]. The high uptake of RERs introduces uncertainties and leads to the voltage fluctuation making the OPF problem more challenging. We formulate the OPF problem into a multi-objective OPF (MO-OPF) optimization problem, in which both uncertain factors and voltage fluctuation control are considered. An overview of the presented work is illustrated in Fig. 1.

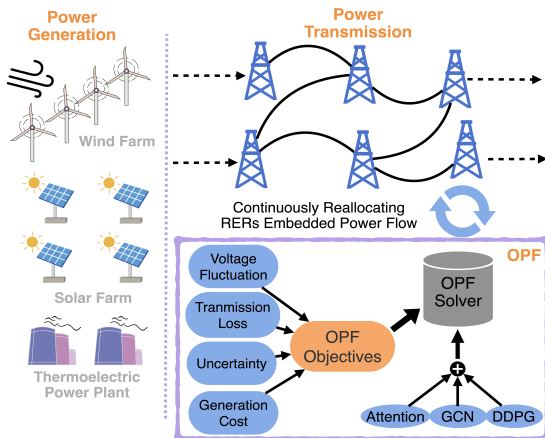


Fig. 1. The system model and the presented work.

### A. Power Generation Cost

The OPF problem usually aims to minimize the power generation cost while satisfying power systems' operating constraints. For fuel energy resources, considering the valve-point effect modeled as a sinusoidal function [10], the generation cost of the  $i$ th thermoelectric generator can be formulated as

$$C_{t,i} = a_i (P_{t,i})^2 + b_i P_{t,i} + c_i + |d_i \sin e_i (e_i (P_{t,i} - P_{t,i}^{\min}))|, \quad (1)$$

where  $P_{t,i}$  and  $P_{t,i}^{\min}$  represent the scheduled and minimal power outputs, respectively, and  $a_i, \dots, e_i$  are constant coefficients.

Due to the intermittent nature of RERs, the cost related to RERs can be divided into two parts: 1) the direct power generation cost [11] and 2) the mismatch cost between scheduled and available power generation [12]. The direct power generation costs for wind and solar PV power are presented, respectively as

$$C_{w,j} = f_j P_{w,j}, \quad (2)$$

$$C_{s,k} = g_k P_{s,k}, \quad (3)$$

where  $f_j$  and  $g_k$  are constant coefficients.

The power mismatch occurs when wind and solar PV power generation are lower or higher than their schedules, resulting in power overestimation or underestimation from uncertain sources, respectively. The variability of RERs can be modeled by an associated probability density function. The power generation cost for power overestimation, namely its reserve cost, can be defined for wind and solar PV power, respectively as

$$C_{w,j}^r = \mathbb{E} [h_{w,j}^r (P_{w,j} - P_{w,j}^a)] \quad (4)$$

$$= h_{w,j}^r \int_{P_{w,j}^a}^{P_{w,j}} (P_{w,j} - p_{w,j}) f_w(p_{w,j}) d(p_{w,j}),$$

$$C_{s,k}^r = \mathbb{E} [h_{s,k}^r (P_{s,k} - P_{s,k}^a)] \quad (5)$$

$$= h_{s,k}^r \int_{P_{s,k}^a}^{P_{s,k}} (P_{s,k} - p_{s,k}) f_s(p_{s,k}) d(p_{s,k}),$$

where  $h_{w,j}^r$  and  $h_{s,k}^r$  represent constant coefficients.

On the contrary, under power underestimation circumstance, if there is no mechanism to reduce power generation from thermoelectric generators, the redundant power generation will be curtailed. We define penalty costs for wind and solar PV power, respectively as

$$C_{w,j}^p = \mathbb{E} [h_{w,j}^p (P_{w,j}^a - P_{w,j})], \quad (6)$$

$$C_{s,k}^p = \mathbb{E} [h_{s,k}^p (P_{s,k}^a - P_{s,k})], \quad (7)$$

where  $h_{w,j}^p$  and  $h_{s,k}^p$  are defined as constant coefficients.

### B. Voltage Fluctuation Control

Voltage fluctuation occurs in power systems especially in the presence of RERs, which greatly degrades the performance of electronic equipment and poses potential security risks on consumers. To mitigate voltage fluctuations, we consider voltage control with metric  $F$  defined as.

$$F = \sum_{j=1}^N \left| V_j^{t_0} - \frac{1}{T_{td}} \sum_{t=1}^{T_{td}} V_j^{t_0-t} \right|, \quad (8)$$

to describe nodes' voltage stability. In Eq. (8),  $N$  represents the number of buses in the given power system, including all power generators, and  $V_j^{t_0}$  is the  $j$ th bus voltage at  $t_0$ .

### C. Power Loss

Transmitting power to consumers inevitably leads to power losses in power systems, and the power losses can be formulated as

$$L = \sum_{b=1}^{N_b} G_{i,j} [V_i^2 + V_j^2 - 2V_i V_j \cos(\delta_{ij})], \quad (9)$$

where  $N_b$  is the total number of branches in the power system,  $\delta_{ij} = \delta_i - \delta_j$  represents the voltage angle difference between the  $i$ th and  $j$ th buses, and  $G_{i,j}$  is the transfer conductance of the  $b$ th branch connecting the  $i$ th and  $j$ th buses.

### D. MO-OPF Formulation

To minimize power generation cost, mitigate voltage fluctuation, and reduce power loss, we consider them as three objectives of the MO-OPF optimization problem defined in Eq. (10)-(12).

$$\min \sum_{i=1}^{N_i} C_{t,i} + \sum_{j=1}^{N_w} (C_{w,j} + C_{w,j}^r + C_{w,j}^p) \quad (10)$$

$$+ \sum_{k=1}^{N_s} (C_{s,k} + C_{s,k}^r + C_{s,k}^p), \quad (11)$$

$$\min F, \quad (11)$$

$$\min L. \quad (12)$$

The above objectives are subject to physical constraints that ensure the safe operation of power systems, formulated as

$$P_{gi} - P_{li} = V_i \sum_{b=1}^{N_b} V_j (G_{i,j} \cos \delta_{ij} + B_{i,j} \sin \delta_{ij}), \quad (13)$$

$$Q_{gi} - Q_{li} = V_i \sum_{b=1}^{N_b} V_j (G_{i,j} \sin \delta_{ij} + B_{i,j} \cos \delta_{ij}), \quad (14)$$

$$\underline{P}_i \leq P_i \leq \bar{P}_i, \quad i = 1, \dots, N, \quad (15)$$

$$\underline{Q}_i \leq Q_i \leq \bar{Q}_i, \quad i = 1, \dots, N, \quad (16)$$

$$\underline{V}_i \leq |V_i| \leq \bar{V}_i, \quad i = 1, \dots, N, \quad (17)$$

$$|\mathbb{S}_b| \leq \bar{S}_b, \quad b = 1, \dots, N_b, \quad (18)$$

where  $\bar{P}_i$  and  $\bar{Q}_i$  are the maximal active and reactive power of the  $i$ th bus, respectively, and  $\bar{S}_b$  represents the maximal apparent power on the  $b$ th branch. Note that both  $V_i$  and  $S_b$  are complex numbers of voltage and apparent power, respectively.

## III. METHODOLOGY

In this section, we propose a DRL-based algorithm to solve the MO-OPF problem described in Eq. (10)-(18), which is reformulated into a Markov decision process (MDP). DDPG is then adopted to solve the derived MDP for its state-of-the-art performance among various DRL algorithms. Moreover, the MG-ASTGCN is introduced to fully extract ST information in power systems, which assists the learning in the sequential DDPG for better performance.

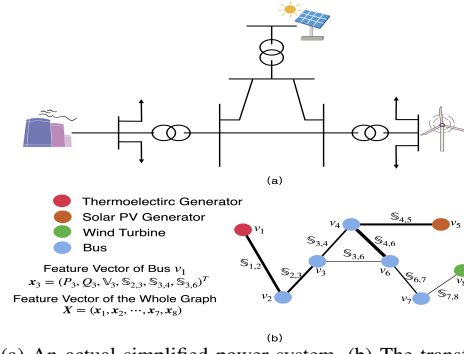


Fig. 2. (a) An actual simplified power system. (b) The transformed graph. A. Spatial-Temporal Correlations Extraction via MG-ASTGCN

1) Preliminaries of MG-ASTGCN: Power system can be modeled as an undirected graph  $\mathcal{G} = (\mathcal{V}, \mathcal{E}, \mathcal{A})$ , as illustrated in Fig. 2. Each node  $v_i$  generates a feature vector  $\mathbf{x}_i$  for gathering local stationary information in each time interval, as formulated in Eq. (19). The aggregate form of feature vector of  $\mathcal{G}$  is shown in Eq. (20).

$$\mathbf{x}_i = (P_i, Q_i, V_i, S_{i,j_1}, S_{i,j_2}, \dots)^T, \quad (19)$$

$$\mathbf{X} = (\mathbf{x}_1, \mathbf{x}_2, \dots, \mathbf{x}_N). \quad (20)$$

Considering periodic patterns in power flow [1], e.g., daily and weekly patterns, a multi-grained vector constructor is developed to better capture temporal correlations of a series of  $\mathcal{G}$ , as shown in Fig. (3), which divided the  $\mathcal{G}$  into recent, daily, and weekly segments as

$$\mathcal{X}_r = \{\mathbf{X}_{t_0-T_r+1}, \dots, \mathbf{X}_{t_0-1}, \mathbf{X}_{t_0}\}, \quad (21)$$

$$\mathcal{X}_d = \{\mathbf{X}_{t_0-T_d \times n_d}, \dots, \mathbf{X}_{t_0-n_d}, \mathbf{X}_{t_0}\}, \quad (22)$$

$$\mathcal{X}_w = \{\mathbf{X}_{t_0-7 \times T_w \times n_d}, \dots, \mathbf{X}_{t_0-7 \times n_d}, \mathbf{X}_{t_0}\}, \quad (23)$$

where  $T_s$ ,  $T_d$ ,  $T_w$  indicate the length of recent, daily, and weekly segments, respectively, and  $n_d$  represents the frequency of adjusting power flow per day.

The framework of the proposed MG-ASTGCN is illustrated in Fig. 3, including graph transformation operation, multi-grained vector constructor, and ASTGCN. ASTGCN is introduced to take multi-grained segments defined in Eq. (21)-(23) as inputs, in which each segment passes through several ST components for ST information extraction. The structure of one ST component is illustrated in Fig. 4.

2) Spatial-Temporal Attention Mechanism: The ST attention mechanism is conducted before graph convolution, as shown in Fig. 4. The idea is to pay more attention to valuable graphical information in both spatial and temporal perspectives on  $\mathcal{G}$  for the sequential convolution operations, which can be considered as graph preprocessing.

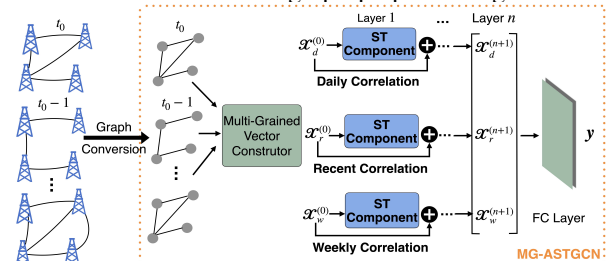


Fig. 3. The framework of the proposed MG-ASTGCN.

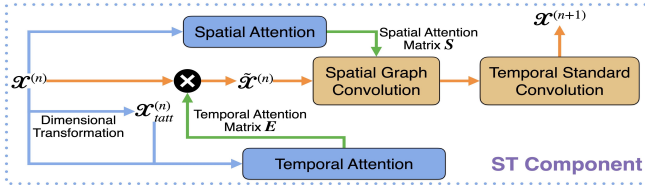


Fig. 4. The structure of one ST component.  $\mathcal{X}^n$  is the output of the previous ST component while  $\mathcal{X}^{n+1}$  represents the input for the next ST component.

**Spatial Attention:** Mutual influence between each node and its neighboring nodes varies dynamically due to changes of power flows. Hence, an attention mechanism in spatial dimension is developed to capture the dynamic correlations among nodes [13], which can be formulated as

$$\mathbf{S} = \mathbf{V}_s \odot \sigma \left[ (\mathcal{X}^{n-1} \mathbf{W}_t)^T \mathbf{W}_{\text{qk}} (\mathbf{W}_f \mathcal{X}^{n-1})^T + \mathbf{b}_s \right], \quad (24)$$

$$s'_{i,j} = \frac{\exp(s_{i,j})}{\sum_{j=1}^N \exp(s_{i,j})}, \quad (25)$$

where  $\mathbf{V}_s$ ,  $\mathbf{W}_t$ ,  $\mathbf{W}_{\text{qk}}$ ,  $\mathbf{W}_f$ , and  $\mathbf{b}_s$  are all learnable parameters. Note that the sigmoid function  $\sigma(\cdot)$  is employed as the activation function.  $\mathbf{S}$  represents the spatial attention matrix, whose element  $s_{i,j}$ , named attention weight, semantically describes the correlation strength between the  $i$ th and  $j$ th nodes. Besides, its normalized  $\mathbf{S}'$  will be adopted for graph convolution to adjust connection weights among nodes.

**Temporal Attention:** Similar to the above spatial attention, the temporal attention mechanism can be formulated to track temporal correlations of each node's state as

$$\mathbf{E} = \mathbf{V}_e \odot \sigma \left[ (\mathbf{U}_n \mathcal{X}_{\text{tatt}}^{n-1})^T \mathbf{U}_{\text{qk}} (\mathbf{U}_f \mathcal{X}^{n-1}) + \mathbf{b}_e \right], \quad (26)$$

$$e'_{i,j} = \frac{\exp(e_{i,j})}{\sum_{j=1}^{T^{n-1}} \exp(e_{i,j})}, \quad (27)$$

where the temporal attention's input  $\mathcal{X}_{\text{tatt}}^{n-1}$  is the transposed form of  $\mathcal{X}^{n-1}$  for the convenience of matrix multiplication. The element  $e'_{i,j}$  represents the normalized strength of temporal dependency between two graph feature vectors  $\mathbf{X}_{t_0-i}$  and  $\mathbf{X}_{t_0-j}$ . The obtained  $\mathbf{E}'$  is used for adding temporal correlations to the ST component's input  $\mathcal{X}^n$ , as shown in Fig. 4.

3) *Spatial-Temporal Convolution:* The ST convolution consists of spatial graph convolution and temporal standard convolution, aiming to extract ST features, and reduce dimensions of inputs to be applicable for our DRL algorithm.

**Spatial Graph Convolution:** Graph convolution is defined as a convolution operation implemented by using linear operators diagonalizing in the Fourier domain to replace the classical convolution operator [14], which can be expressed as

$$\begin{aligned} \text{ReLU}(g_\theta *_{\mathcal{G}} x) &= \text{ReLU}[g_\theta(\mathbf{L})x], \\ &\approx \sum_{k=0}^{K-1} \theta_k \left[ T_k(\tilde{\mathbf{L}}) \odot \mathbf{S}' \right] x, \end{aligned} \quad (28)$$

where  $\mathbf{L}$  and  $\tilde{\mathbf{L}}$  are  $\mathcal{G}$ 's original and normalized Laplacian matrix,  $*_{\mathcal{G}}$  represents the graph convolution operator,  $g_\theta$  is the convolution filter,  $T_k$  is the  $k$ th order Chebyshev polynomial with  $\theta_k$  referred as its coefficient, and the rectified linear unit (ReLU) is adopted as the activation function.

**Temporal Convolution and Feature Compression:**

According to the procedure in Fig. 4, the standard convolution operation is conducted in the temporal dimension, taking the result of spatial graph convolution as the input, which can be formulated as

$$\mathcal{X}^{n+1} = \text{ReLU} \left\{ h_\theta * \left[ \text{ReLU} \left( g_\theta *_{\mathcal{G}} \tilde{\mathcal{X}}^n \right) \right] \right\}, \quad (29)$$

where  $h_\theta$  is the standard convolution filter.

To apply the results of MG-ASTGCN as prior graphical knowledge for our DRL algorithm, the outputs in different time scales are fused and then fed into a fully-connected neural network layer for compression, as shown in Fig. 3, which can be presented as

$$\mathbf{y} = \text{ReLU} \left\{ \text{Dense} \left[ \text{concat} \left( \mathcal{X}_r^{n+1}, \mathcal{X}_d^{n+1}, \mathcal{X}_w^{n+1} \right) \right] \right\}, \quad (30)$$

where **concat** represents the concatenating operation for the above three outputs, and **Dense** is referred as a fully-connected layer for feature compression.

## B. Solving the MO-OPF Problem via DRL

1) *MDP Modeling:* Solving MO-OPF can be considered as a consecutive decision-making process. We model the developed MO-OPF problem as a dynamic MDP [9], consisting of four parts:  $(\mathcal{S}, \mathcal{A}, \mathcal{P}, \mathcal{R})$ .

**State  $\mathcal{S}$ :** For the  $i$ th node in  $\mathcal{G}$ , its state  $s_i^t$  is the feature vector  $\mathbf{x}_i^t$  in Eq. (19).

**Action  $\mathcal{A}$ :** For each power generator, only its active power  $P_i^t$  and voltage  $V_i^t$  can be controlled. Thus, the action space of the  $i$ th node can be expressed as  $a_i^t = \{P_i^t, V_i^t\}$ .

**Probability  $\mathcal{P}$**  is the probability of a transition to the next state  $s_i^{t+1}$  from the current state  $s_i^t$  taking selected action  $a_i^t$ . In DRL, an action strategy is learned to deal with different states, denoted by  $\pi : \mathcal{S} \rightarrow \mathcal{P}^\pi(\mathcal{A})$ , which maps states to a probability distribution over actions. Note that  $\mathcal{P}^\pi$  is different from  $\mathcal{P}$ , in which the probabilistic strategy  $\mathcal{P}^\pi$  is affected by both the inherent transition probability  $\mathcal{P}$  and the selected actions.

**Reward  $\mathcal{R}$ :** Reward  $r_i^t$  is obtained after taking action  $a_i^t$  at state  $s_i^t$ . The goal of DRL is to maximize the reward by learning an optimal action strategy  $\pi$ . Hence, designing an appropriate reward function  $R$  based on objectives and constraints defined in Eq. (10)-(18) plays a significant role in solving MO-OPF via DRL. In this paper, a reward function  $R(\cdot)$ , composing of 8 sub-reward functions from  $r_1(\cdot)$  to  $r_8(\cdot)$  is proposed to reduce power generation cost, alleviate voltage fluctuation, and satisfy operating constraints in power systems, which are formulated in Eq. (33)-(44). Note that,  $N_g$  is the total number of generators,  $C_{w,j}^{\text{d,r,p}}$  and  $C_{s,k}^{\text{d,r,p}}$  represent the summation of direct, reserve, and penalty cost of power generation for wind and solar PV power, respectively;  $r^l$  is the standard line loss rate, and  $I_i$  is the current value, together with its corresponding thermal limit  $T_i$  [15].

2) *Solving MDP by DDPG:* The objective of DRL is to maximize the expected reward  $\bar{R}_\theta$  based on the action policy  $a = \pi_\theta(s)$ , expressed as

$$\begin{aligned} \bar{R}_\theta &= \mathbb{E}_{a^t \sim \pi, r^t, s^{t+1} \sim \mathcal{N}} [R(\tau)] \\ &= \sum_{\tau} R(\tau) P(\tau | \theta), \end{aligned} \quad (31)$$

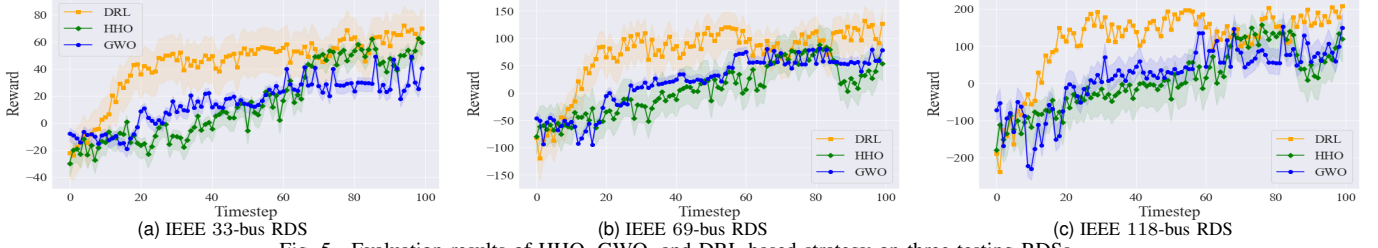


Fig. 5. Evaluation results of HHO, GWO, and DRL-based strategy on three testing RDSs.

where  $\theta$  represents the parameters of  $\pi$ , and  $\tau$  is the trajectory of power flow reallocation, recording all the 4-tuple transitions  $\{s^t, a^t, r^t, s^{t+1}\}$  from the beginning of  $\tau$  to its end. We then introduce DDPG [16] to maximize Eq. (31), where the policy gradient method presented in Eq. (32) is applied in DDPG to update our action policy as

$$\theta \leftarrow \theta - \eta \nabla \bar{R}_\theta. \quad (32)$$

$$R = \sum_{i=1}^8 w_i r_i, \quad r_i \leftarrow \tilde{r}_i, \quad i = 5, 6, 7, \quad (33)$$

$$r_1 = -\sum_{i=1}^{N_t} C_{t,i} - \sum_{j=1}^{N_w} C_{w,j}^{d,r,p} - \sum_{k=1}^{N_s} C_{s,k}^{d,r,p}, \quad (34)$$

$$r_2 = -\frac{1}{r^l} \times \frac{P^l}{\sum_{i=1}^{N_g} P_i}, \quad (35)$$

$$r_3 = 1 - \frac{1}{N_b} \sum_{i=1}^{N_b} \min\left(\frac{I_i}{T_i + \varepsilon}, 1\right), \quad (36)$$

$$r_4 = -F, \quad (37)$$

$$r_5 = \frac{1}{N_g} \begin{cases} \sum_{i=1}^{N_g} \left(1 - \frac{P_i}{\bar{P}_i}\right), & \forall P_i > \bar{P}_i, \\ \sum_{i=1}^{N_g} \left(1 - \frac{P_i}{\underline{P}_i}\right), & \forall P_i < \underline{P}_i, \end{cases} \quad (38)$$

$$\tilde{r}_5 = \exp(r_4) - 1, \quad (39)$$

$$r_6 = \frac{1}{N_g} \begin{cases} \sum_{i=1}^{N_g} \left(1 - \frac{Q_i}{\bar{Q}_i}\right), & \forall Q_i > \bar{Q}_i, \\ \sum_{i=1}^{N_g} \left(1 - \frac{Q_i}{\underline{Q}_i}\right), & \forall Q_i < \underline{Q}_i, \end{cases} \quad (40)$$

$$\tilde{r}_6 = \exp(r_5) - 1, \quad (41)$$

$$r_7 = \frac{1}{N} \begin{cases} \sum_{i=1}^N \left(1 - \frac{|\mathbb{V}_i|}{\bar{V}_i}\right), & \forall |\mathbb{V}_i| > \bar{V}_i, \\ \sum_{i=1}^N \left(1 - \frac{|\mathbb{V}_i|}{\underline{V}_i}\right), & \forall |\mathbb{V}_i| < \underline{V}_i, \end{cases} \quad (42)$$

$$\tilde{r}_7 = \exp(r_6) - 1, \quad (43)$$

$$r_8 = \frac{\sum_{i=1}^{N_w+N_s} P_i}{\sum_{i=1}^{N_w+N_s} \bar{P}_i}. \quad (44)$$

## IV. EXPERIMENTS AND RESULTS

### A. Experimental Settings

The proposed DRL-based strategy is tested on the modified IEEE 33-bus, 69-bus, and 118-bus radial distribution systems (RDSs) [17]. Besides, a workstation with 5 Nvidia TITAN RTX graphics processing units is used for the DRL training.

In our experiments, reward functions defined in Eq. (33)-(44) are adopted to measure the performance of both DDPG and benchmark algorithms. Specifically, we introduce

a criterion to assess algorithms for solving the MO-OPF problem, and the criterion is formulated as

$$\text{SCORE} = \frac{1}{N_{\text{eval}}} \sum_{n=1}^{N_{\text{eval}}} \sum_{t=1}^{T_{\text{end}}} R_n^t, \quad (45)$$

where  $N_{\text{eval}}$  is the number of episodes for evaluation, and  $T_{\text{end}}$  is the length of each episode.

### B. Experimental Results

1) *Comparisons:* Two representative model-based algorithms—harris hawk optimization (HHO) [7] and grey wolf optimization (GWO) [18], are adopted to solve the MO-OPF problem. The evaluation results of these two model-based algorithms, together with the proposed DRL-based strategy on IEEE 33, 69, and 118-bus RDSs are presented in Fig. 5. We see that the proposed DRL-based strategy outperforms other two model-based algorithms. We also find that DRL-based strategy consumes much less time at each timestep while still achieving outstanding performance. The reason for such performance gap is twofold: (i) Model-based algorithms do not need training, resulting in longer computation time at each timestep. Meanwhile, since they tend to get stuck in local optimums, their selected actions are less likely to be the optimal ones, resulting in smaller rewards; (ii) Tremendous data sampled by the DRL-based strategy results in its more effective and efficient searching in the action space. Therefore, DRL reacts much faster at the beginning of evaluation and gradually obtains a higher reward, especially in the large-scale power system, as shown in Fig. 5c.

2) *Effectiveness of the ST Attention:* To evaluate the effectiveness of the ST attention and its impact on the sequential DDPG, the ST attention mechanism is substituted with several other techniques for graphical correlation extraction, including cosine similarity (CS) and jaccard similarity (JS), whose training results are presented in Fig. 6c. We can summarize several observations regarding the effectiveness of the ST attention: 1) The ST attention can dramatically increase DDPG's convergence speed, where more effective searching in the action space is conducted based on the extracted graphical knowledge; 2) It is challenging for a standard DRL algorithm to tackle the complex MO-OPF problem, since both action and state space in RDSs are considerably large; 3) The substituted methods are less effective than the ST attention, since they only focus on degree correlations among different nodes, ignoring both nodes' inner features and temporal dependencies.

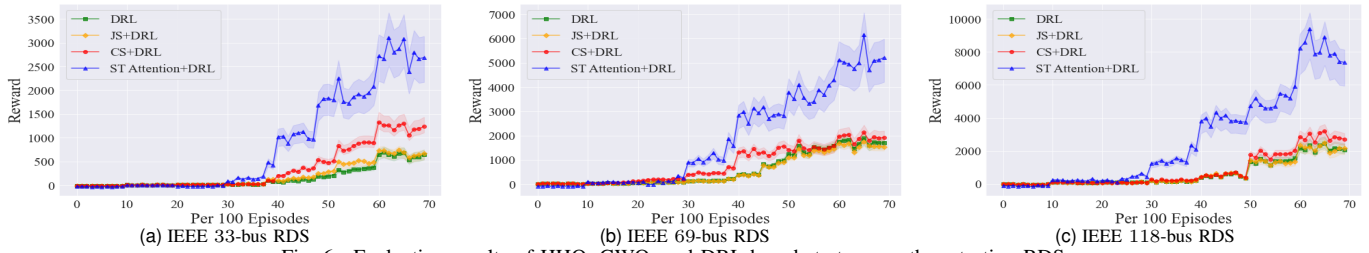
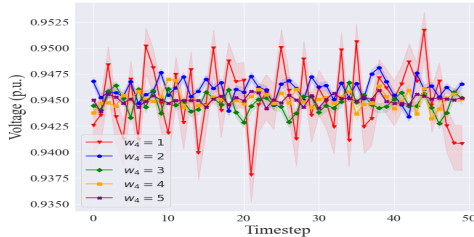


Fig. 6. Evaluation results of HHO, GWO, and DRL-based strategy on three testing RDSS.



$w_4$	SCORE in 33-bus RDS	SCORE in 69-bus RDS	SCORE in 118-bus RDS
1	<b>4014.59</b>	<b>7756.64</b>	<b>14384.11</b>
2	3979.14	7544.81	13958.24
3	3967.51	7394.53	13572.31
4	3843.72	7252.66	12891.59
5	3687.13	7036.29	12186.67

Fig. 7. The left figure illustrates a case study on voltage fluctuation with different  $w_4$ . The right table shows detailed evaluation results with different  $w_4$ .

3) *Voltage Fluctuation Control*: The weights assigned for each reward function described from Eq. (33) to Eq. (44) represent their corresponding importance. We conduct several experiments with different *voltage fluctuation weight*  $w_4$ , to test the DRL-based strategy’s capability in dealing with voltage fluctuations, as presented in Table 7b. Specifically, Bus 15’s voltage fluctuation in IEEE 69-bus RDS is presented in Fig. 7a. Interestingly, although the voltage fluctuation is well-controlled with the increase of  $w_4$ , as shown in Fig. 7a, our DRL-based strategy seems to get stuck in local optima, i.e., SCOREs with  $w_4$  from 2 to 4 are lower than  $w_4$  initialized as 1. Moreover, we find that the performance of DRL-based strategy degenerates with larger  $w_4$ , when it comes to large-scale power systems. The proposed DRL-based strategy will find the sub-optimal power flow, if voltage fluctuation control is overemphasized.

## V. CONCLUSIONS

In this paper, we proposed a DRL-based strategy, accompanied by multi-grained ST graph information, to solve the MO-OPF problem in power systems with a high uptake of RERs. The aim is to alleviate uncertainties brought in by RERs and improve power systems’ stability for solving the OPF problem more effectively and efficiently. We can draw several conclusions based on our experimental results: (i) Extracting ST correlations in power systems plays an essential role in solving the MO-OPF problem. (ii) Compared with two benchmark model-based algorithms, the proposed DRL-based strategy achieves better performance in solving the OPF problem with less computational time.

## REFERENCES

- [1] L. Ranalder, H. Busch, T. Hansen, M. Brommer, T. Couture, D. Gibb, F. Guerra, J. Nana, Y. Reddy, J. Sawin, K. Seyboth, and F. Sverrisson, *Renewables in Cities 2021 Global Status Report*. REN21 Secretariat, Mar. 2021.
- [2] S. S. Reddy, “Optimal power flow with renewable energy resources including storage,” *Electrical Engineering*, vol. 99, pp. 685–695, 6 2017.
- [3] S. Impram, S. Varbak Nese, and B. Oral, “Challenges of renewable energy penetration on power system flexibility: A survey,” *Energy Strategy Reviews*, vol. 31, p. 100539, 2020.
- [4] J. Carpentier, “Optimal power flows,” *International Journal of Electrical Power & Energy Systems*, vol. 1, no. 1, pp. 3–15, 1979.
- [5] B. Li, W. Wang, Y. Liu, B. Li, and W. Wen, “Research on power flow calculation method of true bipolar vsc-hvdc grids with different operation modes and control strategies,” *International Journal of Electrical Power & Energy Systems*, vol. 126, p. 106558, 03 2021.
- [6] P. Siano, C. Cecati, H. Yu, and J. Kolbusz, “Real time operation of smart grids via fcn networks and optimal power flow,” *IEEE Transactions on Industrial Informatics*, vol. 8, pp. 944–952, 2012.
- [7] M. A. M. Shaheen, H. M. Hasanien, S. F. Mekhamer, and H. E. A. Talaat, “Optimal power flow of power networks with penetration of renewable energy sources by harris hawks optimization method,” in *2020 2nd International Conference on Smart Power Internet Energy Systems (SPIES)*, 2020, pp. 537–542.
- [8] X. Lei, Z. Yang, J. Yu, J. Zhao, Q. Gao, and H. Yu, “Data-driven optimal power flow: A physics-informed machine learning approach,” *IEEE Transactions on Power Systems*, vol. 36, pp. 346–354, 1 2021.
- [9] R. S. Sutton and A. G. Barto, *Reinforcement Learning: An Introduction*. Cambridge, MA, USA: A Bradford Book, 2018.
- [10] H. Bouchekara, A. Chaib, M. Abido, and R. El-Sehiemy, “Optimal power flow using an improved colliding bodies optimization algorithm,” *Applied Soft Computing*, vol. 42, pp. 119–131, 05 2016.
- [11] P. P. Biswas, P. N. Suganthan, and G. A. Amaratunga, “Optimal power flow solutions incorporating stochastic wind and solar power,” vol. 148, pp. 1194–1207, 2017.
- [12] A. Panda and M. Tripathy, “Security constrained optimal power flow solution of wind-thermal generation system using modified bacteria foraging algorithm,” *Energy*, vol. 93, pp. 816–827, 12 2015.
- [13] A. Vaswani, N. Shazeer, N. Parmar, J. Uszkoreit, L. Jones, A. N. Gomez, L. u. Kaiser, and I. Polosukhin, “Attention is all you need,” in *Advances in Neural Information Processing Systems*, I. Guyon, U. V. Luxburg, S. Bengio, H. Wallach, R. Fergus, S. Vishwanathan, and R. Garnett, Eds., vol. 30. Curran Associates, Inc., 2017.
- [14] S. Zhang, H. Tong, J. Xu, and R. Maciejewski, “Graph convolutional networks: a comprehensive review,” *Computational Social Networks*, vol. 6, no. 1, p. 11, Nov 2019.
- [15] J. D. D. Glover and M. S. Sarma, *Power System Analysis and Design*, 3rd ed. USA: Brooks/Cole Publishing Co., 2001.
- [16] T. P. Lillicrap, J. J. Hunt, A. Pritzel, N. Heess, T. Erez, Y. Tassa, D. Silver, and D. Wierstra, “Continuous control with deep reinforcement learning,” 2019.
- [17] J. Li, R. Zhang, H. Wang, Z. Liu, H. Lai, and Y. Zhang, “Deep reinforcement learning for optimal power flow with renewables using spatial-temporal graph information,” 2021.
- [18] I. U. Khan, N. Javaid, K. A. Gamage, C. J. Taylor, S. Baig, and X. Ma, “Heuristic algorithm based optimal power flow model incorporating stochastic renewable energy sources,” *IEEE Access*, vol. 8, pp. 148 622–148 643, 2020.